Micropolarity and Order in the Reverse Micelles of L62 and L64 Pluronic Copolymers, As Studied by Molecular Probe Techniques

Marilena Vasilescu,* Agneta Caragheorgheopol, Horia Caldararu,* and Rodica Bandula

"I.G.Murgulescu" Institute of Physical Chemistry, Romanian Academy, Splaiul Independentei 202, 77208 Bucharest, Romania

Helge Lemmetyinen

Institute of Materials, Tampere University of Technology, P.O. Box 541, FIN-33101 Tampere, Finland

Heikki Joela

Department of Chemistry, University of Jyvaskyla, P.O. Box 35, SF-40351 Jyvaskyla, Finland

Received: April 21, 1998

The reverse micelles of triblock copolymers poly(ethylene oxide)-*block*-poly(propylene oxide)-*block*-poly(ethylene oxide) $EO_6PO_{36}EO_6$ (Pluronic L62) and $EO_{13}PO_{30}EO_{13}$ (Pluronic L64) in ternary (copolymer/*o*-xylene/water) and binary (copolymer/water) systems with different water contents were evidenced and investigated by fluorescence, absorption, and spin probe techniques. The spectral parameters of the polarity sensitive probes, 1-anilinonaphthalene-8-sulfonic acid (ANS), dansylhexadecylamine (Dansyl), pyrenesulfonic acid (PSA), 4-nitropyridine *N*-oxide (NP) and 4-(*N*,*N*′-dimethyl-*N*-alkyl)ammonium 2,2′,6,6′-tetramethylpiperidine-1-oxyl iodide (CAT *n*), were related to the local hydration and polarity by comparison with a series of poly(oxyethylene)/water (TEG/water) calibration mixtures. The data were concordant and complementary, resulting in polarity profiles of the core for all systems and the relative radial positioning of the probes. The order of decreasing hydrophobic character found was Dansyl > NP > CAT 16 > CAT 11 ∼ ANS > CAT 8 > PSA > CAT 4 > CAT 1. A linear relationship was found between the R_A (the intensity ratio of two absorption vibronic bands) of PSA in ethanol/water mixtures and Kosower's *Z* parameter ($Z = -29.0R_A + 177.83$). Thus, by means of the calibration mixtures, converting different spectral parameters of the mentioned probes, the local polarity values were expressed in terms of *Z* values. The role of water as a prerequisite for micellization was evidenced and so was the minimum quantity of water required in the ternary systems ($W = 0.2$ for L64 and $W = 0.4$ for L62). Regarding the water distribution, a more advanced segregation of water is observed in the ternary systems as compared to the binary ones, pointing to the role played by the solvent in this process. Evidence was found for a considerable solvation of the poly(propylene oxide) block with xylene, leading to a looser packing in the corona and in the poly(ethylene oxide) core. In the case of ternary systems, the ordering of the polymer chains in the micelles, measured with a series of *x*-doxylstearic acid spin probes, indicates the progress of micellar organization with increasing water content, the order increasing and extending further from the polar core and the corona becoming less penetrable. In the corresponding binary systems, the polymer chain rotation is "frozen" at room temperature (295 K) and even at 320 K. The structural characteristics of L62 and L64 ternary systems are rather similar, a conclusion suggested especially by the information the polar probes supplied. There are differences in the microenvironment of more hydrophobic probes, which sense a higher hydrophobicity in the case of L62, the increase of microviscosity being also more marked in the L62 system.

Introduction

The triblock copolymers poly(ethylene oxide)-*block*-poly(propylene oxide)-*block*-poly(ethylene oxide), (PEO−PPO−PEO), commercial name Pluronics, has been given considerable attention owing to their applications in industry (detergents, stabilizers, emulsifiers, cosmetics, drugs) and to their amphiphilic behavior in solutions, leading to complex self-assembled structures in various environments. It is well-known that these copolymers form micelles in water at certain concentrations and temperatures (see the reviews, in refs 1−4). Their size and shape depend on temperature, pressure, concentration, additives, and block copolymer compositions. The behavior of Pluronic block copolymers in nonaqueous solvents enjoyed much less attention.[5−9] These triblock copolymers and poly(ethylene glycol) alkyl ether nonionic surfactants possess the same hydrophilic moiety (PEO). The nonionic surfactants mentioned may form micelles in nonpolar solvents, and water addition plays a very important role in micellization.[2,10−14] The colloidal behavior of triblock copolymers in nonaqueous media

S1089-5647(98)01932-4 CCC: $15.00
Published on Web 09/17/1998

could be similar, but the information available in the literature is scarce. Therefore, problems such as the formation of micelles in nonpolar solvents and the influence of water addition upon micellization are very important and up-to-date. In the case of the L64/*o*-xylene/water system, the phase diagram[7] and several studies of light,[6] small-angle X-ray,[7−9] and neutron scattering[15] are available. These studies focus on the micelle structure and the effect of water addition in the L64/*o*-xylene system. The reverse micellar phases of L64 in *o*-xylene were studied by ESR spectroscopy on a set of cationic spin probes.[16] The conclusion was reached that the presence of water is essential for the association in the reverse micelles, with PEO blocks and water forming the polar core and the middle block (PPO) extending into the apolar environment. It was also found out that water has a nonuniform distribution in the polar core, being concentrated toward the micellar center. The hydration gradient was established in comparison with TEG/water calibration mixtures.

Regarding L62, the data in the literature are even scarcer,[17−19] and no study was issued yet on reverse micelles. Moreover, even for the L64 reverse system, data on the polarity profile in regions of the micelles farther from the polar core are not available. This is why a more comprehensive study of both L62 and L64 reverse systems has been undertaken, using a variety of molecular (fluorescence, absorption UV−vis and spin) probes, aiming at obtaining information on the micellization process and a detailed polarity profile. Referring all data to a common polarity scale (Kosower's *Z*) was also intended as in a previous study on Triton X-100 reverse micelles.[14] Also, data on the surfactant packing in the aggregates—by measuring the local viscosity and the order degree of the surfactant chains—and how these parameters are affected by hydration and solvent (*o*-xylene) have been aimed at.

Experimental Section

Materials. Pluronic L62 $(EO)_6(PO)_{36}(EO)_6$ (MW = 2600) and Pluronic L64 $(EO)_{13}(PO)_{30}(EO)_{13}$ (MW = 2900) were obtained from BASF and used without purification. The poly(ethylene oxides) employed for calibration were as follows: Carbowax 200 (poly(ethylene glycol) 200, TEG), average molecular weight 200 (Loba Chemie), triethyleneglycol monomethyl ether (TGMME) (Fluka), tetraethyleneglycol dimethyl ether (TEGDME) (Aldrich), and poly(propylene glycol) (PPO), average molecular weight 2000 (Aldrich). The water content determined by Karl Fischer titration was 0.34% (w/w) in pluronic L64, 0.4% (w/w) in TEG, 0.12% (w/w) in TGMME, and 1% (w/w) in TEGDME. The *o*-xylene (BDH) was dried on molecular sieves; the water content in the dry product was 0.015% (w/w). Use has been made of deionized or double-distilled water.

The fluorescence probes, 1-anilinonaphthalene-8-sulfonic acid (ANS), *N*-[5-(dimethylamino)naphthalene-1-sulfonyl]hexadecylamine (Dansyl) and pyrenesulfonic acid sodium salt (PSA), all of special purity, were supplied by Molecular Probes, Eugene, OR. PSA was also employed as an UV−vis absorption probe together with 4-nitropyridine *N*-oxide (NP) (content > 97%; Aldrich).

Two series of nitroxide spin probes were used: 4-(*N*,*N*′-dimethyl-*N*-alkyl)ammonium 2,2′,6,6′- tetramethylpiperidine-1-oxyl iodide (CAT *n*), with *n* being the number of carbon atoms in the alkyl substituent equal to 1, 4, 8, 11, and 16 (Molecular Probes), and *x*-doxylstearic acid (*x*-DSA) with *x*, the carbon atom to which the doxyl group is attached, being equal to 5, 7, 10, and 16 (Sigma Chemical Company). All probes were used as received.

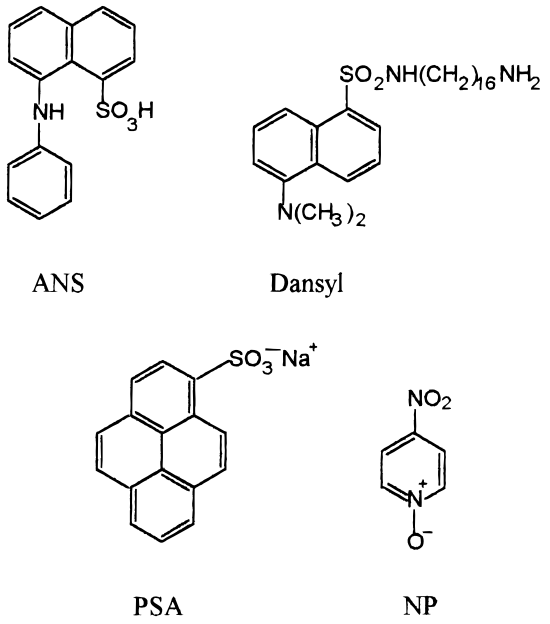

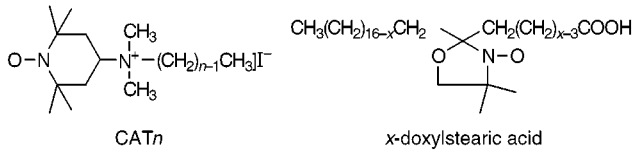

Preparation of Samples. The polymer concentration in *o*-xylene was 34.5% (w/w) for both L62 and L64, which corresponds to one of the samples investigated by Chu et al. in the case of L64,[3,5] the one which dissolves the greatest amount of water. The phase diagrams for L64/*o*-xylene/water[7] and for L62/*o*-xylene/water[20] support the assignment of the investigated samples as belonging to the L_2 phase. The solutions, prepared by solving the copolymers in *o*-xylene, were stored 24 h before measurements. The amounts of added water were expressed as $W = [H_2O]/[EO]$ molar ratios. Binary copolymer/water systems were also prepared. Their concentrations were 92.3% (w/w) ($W = 1$) and 85.8% (w/w) ($W = 2$) for L62 and 86.1% (w/w) ($W = 1$) for L64 (also in the L_2 phase[7]). Solutions were stored several days to ensure homogenization.

The molecular probes were dissolved in ethanol and stock solutions were obtained, of which adequate amounts were taken and thoroughly evaporated on the walls of a flask by means of a nitrogen stream. Afterward, the sample solutions were added and, after 5 min of stirring, were left overnight to ensure the solubilization of the probe. The final concentrations of the fluorescence probes were 1×10^{-5} M for the Dansyl and ANS probes and 5×10^{-6} M for PSA. In the case of the UV−vis absorption probes, the final concentrations were 1×10^{-4} M for NP and 5×10^{-4} M for PSA. The spin probe concentrations were within the 1×10^{-4}−5×10^{-4} M range.

Calibration Procedures. For each type of spectroscopic measurement, the values of the polarity-sensitive parameter were "translated" into local hydration values by means of calibration curves representing the variation of the corresponding parameter in a set of TEG/water mixtures with different *W* values. Thus, local hydration values (W_{eff}) are obtained for the location of each probe in the micelles. For the NP and PSA absorption probes, a linear dependence of the spectral parameters on Kosower's *Z* parameter was established by measurements in a

series of polar solvents and used to assign the *Z* values to TEG, TGMME, and TEGDME/water mixtures.

Fluorescence Measurements. The fluorescence spectra were recorded on a Shimadzu RF 5000 spectrophotometer. Time-resolved fluorescence decay measurements were carried out using an Edinburg Instrument 199 single-photon counting fluorescence time-domain spectrofluorometer interfaced to an IBM-compatible computer.[12] The instrumental response function was recorded separately at the wavelength of the exciting pulse. The fluorescence lifetimes have been calculated making use of IBM software including reconvolution fitting programs. The measurements were carried out at 296 K for steady-state measurements and at 293 K for lifetime measurements.

UV−Vis Measurements. The absorption spectra were recorded by means of a Shimadzu 2501 PC spectrophotometer at 296 K with an accuracy of 0.2 nm in 1-cm silica cells. The absorption of NP at λ_m in the surfactant solutions obeys the Bougner−Lambert−Beer rule over the concentration range investigated.

ESR Measurements. The ESR spectra were recorded on a JES-3B (JEOL) spectrometer and on a ESP 300 (Bruker) spectrometer with 100-kHz field modulation using X-band frequency. The ^{14}N isotropic hyperfine splitting, a_N, the polarity-sensitive parameter,[21] was measured in comparison with that of Fremy's salt ($a_N = 13.0$ G). The isotropic rotational correlation time, τ_c, was calculated from the line heights ratio as previously described.[22] τ_c is connected to the local viscosity, η, by the Debye−Stokes−Einstein equation: $\tau_c = 4\pi\eta R^3/3kT$, where R is the hydrodynamic radius of the tumbling entity. The order parameter, S, is defined in terms of observed spectral parameters as[23]

$$S = \frac{A_{||} - A_{\perp}}{A_{zz} - (A_{xx} + A_{yy})/2}$$

where A_{zz}, A_{xx}, and A_{yy} are the principal elements of the $\boldsymbol{A}$ tensor in the absence of molecular motion and $A_{||}$ and $A_{\perp}$ are derived from experimental spectra. The order parameters corrected for polarity differences and errors in reading the $A_{\perp}$ values were calculated using the following parameters reported for the doxyl probes:[24] $A_{zz} = 33.5$ G, $A_{xx} = 6.3$ G, and $A_{yy} = 5.8$ G. The quenching experiments with the paramagnetic line broadening agent CuX_2, where X = 1-methyl-2-carbethoxyglyoxal-*p*-tolylanil-(1)-*m*-tolylhydrazone-(2), have been performed as indicated elsewhere.[25]

Results and Discussion

Fluorescence. *ANS Probe*. 1-Anilinonaphthalene-8-sulfonic acid belongs to the class of (arylamino)naphthalenic derivatives which present a red shift of the fluorescence band and a decrease of quantum yield with increasing polarity. The best explanation of the ANS fluorescence complex behavior is that based on the model of solute−solvent interaction (see the review in ref 26). Compared to naphthalene, the attachment to the aromatic ring system of the two groups which are, respectively, a good electron donor (arylamino group) and a good electron acceptor (S═O group) produces, when excited, besides the singlet state S^*_1, a lower excited state with an important charge-transfer character, $S^*_{1,CT}$. Emission can occur from either of these two states, the yields of $S^*_1 \rightarrow S^*_{1,CT}$ and $S^*_{1,CT} \rightarrow S_0$ processes being controlled by both the viscosity of the medium and its polarity.[26,27] The effect of the solvent's physical properties (polarity, viscosity) on the fluorescence emission of ANS has also been explained in terms of the assumption of two different conformations, having the benzene ring coplanar and noncoplanar with the naphthalene plane.[27,28] The intramolecular interaction between the *peri* substituents in ANS, which is strongly influenced by the solvents, may indeed determine a deviation from planarity.[28,29] ANS fluorescence is strongly quenched in water to give yields in the range 0.003−0.011, compared with 0.40 in methanol.[30] The quenching effect of water arises mainly from the flexibility of the ANS molecule in water. The solvents (alcohols) that favor intramolecular hydrogen bonds between the NH and SO_3^- groups favor formation of the coplanar conformation. Increased viscosity enhances the fluorescence emission, mainly by increasing the molecular rigidity, favoring coplanar configuration.[28]

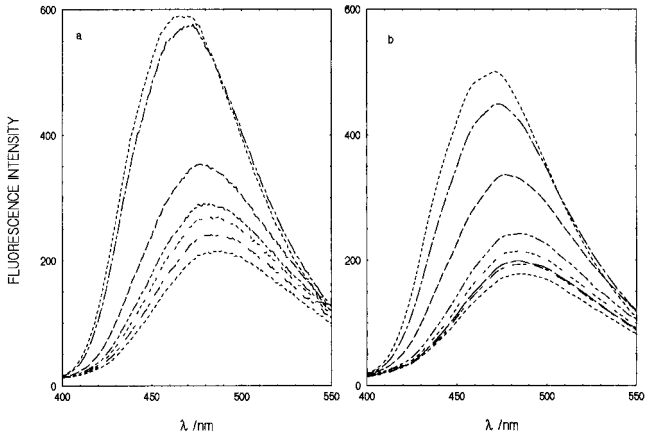

Figure 1. Fluorescence spectra of the ANS probe in L62/*o*-xylene/water (a) and in L64/*o*-xylene/water (b) solutions with various W; $\lambda_{ex} = 335$ nm; from top to bottom, the spectra are as follows: (a) $W = 0$, 0.1, 0.4, 0.6, 0.8, 1.4, and 2.5; (b) $W = 0$, 0.1, 0.2, 0.5, 0.7, 1.0, 1.6, and 2.

The corrected fluorescence spectrum of ANS exhibits a wide band whose maximum shifts from 465.8 nm in *o*-xylene to 554.9 nm in water. Parts a and b of Figure 1 show the fluorescence spectra of ANS in the L62/*o*-xylene/water and L64/*o*-xylene/water systems at different water contents, W; note the red shift of the fluorescence band and the fluorescence decrease in intensity with increasing W values. Table 1 lists the positions of the ANS fluorescence band maxima, λ_m, in the studied systems, reference mixtures, and various solvents. The fluorescence intensity jump (as one can note in Figure 1) and the significant shift of λ_m at $W = 0.2$ for L64/*o*-xylene and at $W = 0.4$ for L62/*o*-xylene are assigned to the formation of the micelles, where the probe experiences a much greater polarity, as compared to the solvent. The λ_m values measured in the micelles compared to the reference mixtures afford the assignment of the probe localization in the hydrophilic intramicellar part, more precisely in the region of oxyethylenic chains, since the polarity is equivalent to that of TEG/water mixtures with different water contents.

The shape of the fluorescence band suggests that it might originate from the overlap of two bands. Thus, the fluorescence bands have been analyzed by means of a deconvolution program (Peakfit). Table 1 lists the positions of the maxima (λ_1 and λ_2) of the Gaussian bands separated, as well as the fluorescence intensity ratios, R_F, of these bands. We have assigned these two bands to the two geometrical forms, planar and nonplanar, of the ANS molecule. The proportion and positions of the bands depend on the solvent properties. It is worth mentioning that in the solvents studied (TEG, PPO, *o*-xylene), the intensities of the two bands are comparable (the ratio ranges within 1.31−

TABLE 1: Fluorescence Parameters of the ANS Probe in Various Reference Solutions and in Reverse Micelles of L62 and L64 in *o*-Xylene as a Function of $W = [H_2O]/[EO]$; $\lambda_{ex} = 335$ nm[a]

system	W	λ_m, nm	λ_1, nm	λ_2, nm	R_F	τ_1, ns	τ_2, ns
o-xylene		465.8	458.5	482.0	1.13		
TEG/H_2O	0	481.1	480.2	510.9	1.31	12.15	2.01
	0.2	484.2	482.3	542.6	3.70	10.80	2.29
	0.4	487.0	484.5	544.9	4.09	9.65	1.97
	0.7	489.8	488.8	548.3	4.69	7.72	1.69
	1.0	491.4	491.7	549.6	5.96	6.35	1.55
PPO	0	466.1	454.7	489.02	1.20		
L62/*o*-xylene/	0	467.7	455.6	490.4	1.24	10.40	2.35
H_2O	0.1	469.5	457.9	493.5	1.26	10.63	2.02
	0.2	472.7	460.4	496.7	1.32	10.74	1.94
	0.4	477.7	475.9	538.7	4.42	11.00	2.03
	0.5	480.4	480.8	545.5	6.09	9.20	1.98
	0.6	482.3	482.7	547.3	6.77		
	0.7	482.3	483.9	546.1	7.64	8.52	1.32
	1.0	483.8	485.5	546.7	7.95	8.23	1.22
	1.2	484.8	485.9	546.4	8.10		
	1.4	485.1	486.5	548.0	8.49	7.98	1.43
	2.0	485.1	487.1	546.8	8.88	7.81	1.36
	2.5	486.1	487.6	547.4	9.33		
	3.0	486.4	488.0	546.1	10.10	7.64	1.26
	3.9	486.6	488.3	548.0	11.32	7.70	2.12
L64/*o*-xylene/	0.0	471.7	458.9	495.0	1.51	10.98	2.77
H_2O	0.1	472.9	464.0	502.7	1.78	11.02	2.62
	0.2	477.9	478.9	546.9	7.26	10.85	2.29
	0.5	485.7	484.9	549.0	7.92	9.82	1.99
	0.7	484.8	484.9	547.4	8.81	8.35	1.60
	1.0	484.5	485.8	547.9	7.43	8.35	1.60
	1.6	485.1	488.9	547.9	8.60	7.43	1.68
	2.0	485.7	487.9	546.7	12.86	7.40	2.00

[a] R_F stands for the intensity ratio of the bands with the maxima at λ_1 and λ_2, respectively; $\lambda_{ex} = 295$ nm and $\lambda_{em} = 480$ nm were employed to measure the fluorescence lifetime.

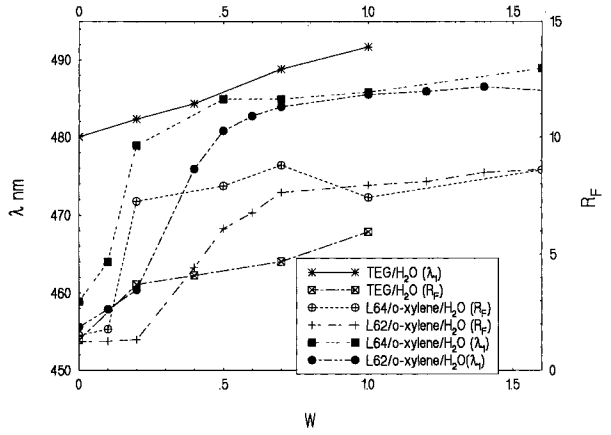

Figure 2. Plot of λ_1 and R_F versus W for the ANS probe in the L62/*o*-xylene/water and L64/*o*-xylene/water systems and TEG/water mixtures.

1.13). Addition of water to TEG decreases the intensities of both bands, affecting the second band to a greater extent, thus yielding an increase of R_F (Table 1). A similar trend for R_F is observed in the case of the L62/*o*-xylene/water and L64/*o*-xylene/water solutions (Figure 2) for which one can note the following: (i) At low water contents ($W < 0.2$) for L62 and ($W < 0.1$) for L64, the intensities of the two bands are comparable. (ii) At W values higher than 0.4 for L62 solutions and higher than 0.2 for L64, a steep increase of the R_F ratios and an abrupt red shift of the band maximum position are recorded (Figure 2). This finding suggests a more polar and more viscous surrounding (the intensity of band 1 increases sensibly, while that of band 2 decreases), which evidences the

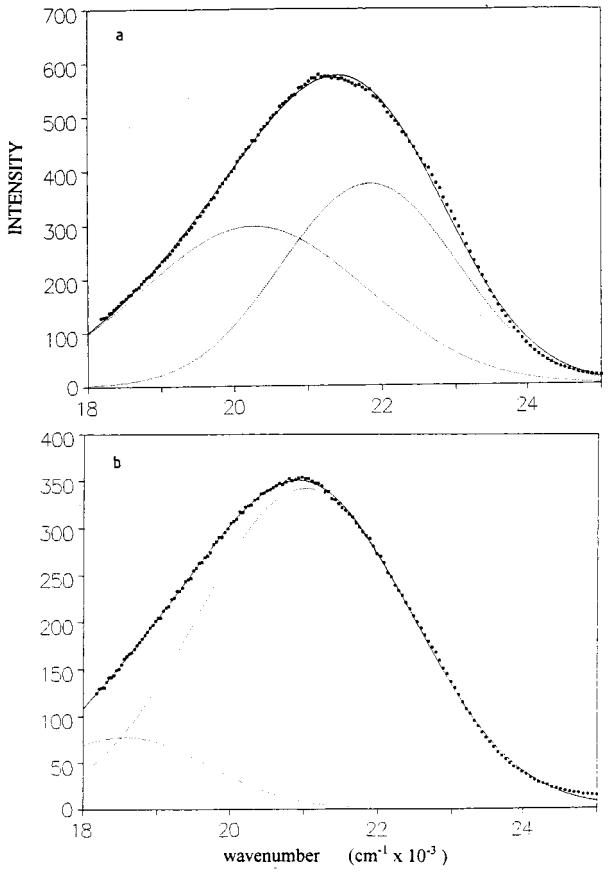

Figure 3. Deconvoluted fluorescence spectrum of ANS in the L62/*o*-xylene/water solution; $W = 0.1$ (a) and 0.4 (b); $\lambda_{ex} = 335$ nm.

formation of micelles. (iii) R_F increases gradually with increasing W so that at high W values, one can consider that there is only one band, that of lower wavelength. The fluorescence intensity of the second band is strongly diminished compared with that of the first band when water is added. These findings are presented in parts a and b of Figure 3 for L62/*o*-xylene at $W = 0.1$ (before micellization) and $W = 0.4$ (after micellization), respectively. The λ_1 and R_F dependences on W (Figure 2) evidence micellization by clear jumps placed at the same W value. A red shift is also noted for λ_2 when W increases, and the shift is more important at micellization (Table 1). The W dependence of R_F also supplies information regarding the variation of viscosity and polarity of the probe microenvironment. The R_F values are higher in micellar solutions compared to TEG/water mixtures (Figure 2), pointing to a higher microviscosity in the micelles, which favors the coplanar geometry of the probe.

The fluorescence lifetime was measured at $\lambda_{em} = 480$ nm, a value close to the maximum of the first band. However, the fluorescence decay is not described by a monoexponential. The results were better fitted to a sum of two exponentials, yielding two lifetime values (Table 1). An example of ANS fluorescence decay curves in the L64/*o*-xylene/water systems with $W = 1.5$ is shown in Figure 4. The values of τ_1 decrease continuously with W in the case of TEG/water solution, while in polymer solutions, in the first region τ_1 is constant followed by a decrease after micellization. This decrease is initially more important owing to the quenching effect of water; then the decrease is continuous, yet very slow, which indicates a segregation of water in a more polar zone.

The values of τ_2 (probably corresponding to the second band) are small, less than 3 *n*s and with a percent weight of less than

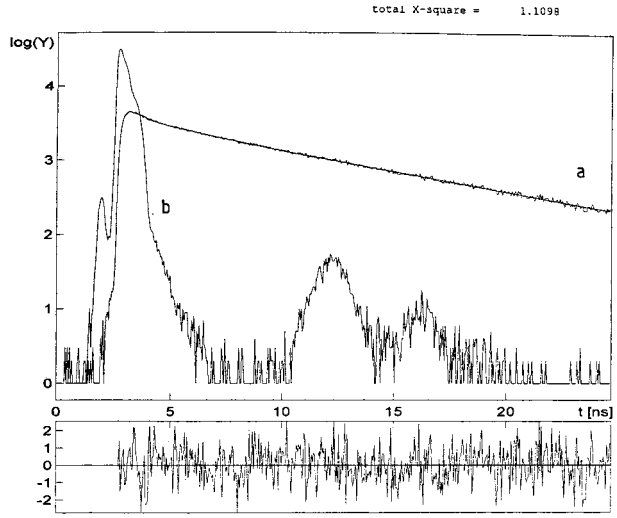

Figure 4. Fluorescence decay curve for ANS in the L62/*o*-xylene/water solution; $W = 1.6$; $\lambda_{em} = 480$ nm (a); the laser decay curve (b).

5%. They also exhibit a tendency to decrease with *W* as a result of the fluorescence quenching action of the water.

All ANS fluorescence parameters clearly show micellization at W = 0.4 for L62/o-xylene and W = 0.2 for L64/o-xylene, followed by a small increase of micropolarity with W at the location of the probe in the micelle, in the poly(oxyethylene) region.

Dansyl Probe. Dansyl, like ANS, is also a naphthalene derivative, whose fluorescence is sensitive to polarity: the fluorescence maximum shifts toward red, while the fluorescence yield decreases with increasing solvent polarity. It is well-known that, in the case of 1-(dimethylamino)-5-naphthalene-sulfonate, which is chemically related to Dansyl, the lowest energy excited state possesses a considerable character of charge transfer (involving the lone-pair electrons of nitrogen). The nature of the lowest energy state, which is an emissive state, depends on solvent polarity.[31] Dansyl, having a long alkyl group in the molecule, is more hydrophobic than ANS, and one expects it to be located in the micelle closer to the PPO region. Table 2 shows the positions of the fluorescence band maxima of Dansyl in the micellar systems and, for comparison, in the reference mixtures and a few solvents. The following behavior is observed (Figure 5 and Table 2): (i) At $W = 0$, for both ternary systems, the probe senses a higher polarity than in *o*-xylene and PPO but one that is lower than that in TEG, TGMME, or TEGDME (solvents that can be considered to mimic the hydrophilic part of the surfactants). (ii) On water addition, λ_m increases considerably, owing to micellization, then only slightly, suggesting the reduced influence of the added water on the local polarity around the probe; even for high *W* values, the λ_m values remain below those of TEG. These data indicate the location of Dansyl near the PPO region. (iii) At $W > 1.1$ for L62 and at $W > 0.7$ for L64, λ_m slightly shifts toward blue, corresponding to a decrease of local polarity. This peculiar behavior may be assigned to a more advanced PEO/PPO block separation (by means of stretching polyoxyethylenic chains upon solvation with water), also yielding more compact micellar aggregates, a fact also supported by other observations which will be discussed further. In the same water composition region, Wu and co-workers[6] observed, by light scattering and NMR, the modification of the spherical shape of the micelles.

The splitting of the Dansyl fluorescence band into two Gaussian components was also attempted, as in the case of ANS. Table 2 lists the maxima of the two bands and the values of the intensity of the first fluorescence band (at λ_1), to evidence the effect of the increasing amounts of water: shifting the wavelength and decreasing the fluorescence intensity. R_F is much higher than for ANS, more so in micellar solutions. A considerable increase of R_F at micellization was observed; e.g., in the case of L62/*o*-xylene/water, R_F increases from 3.81 (*W*

TABLE 2: Fluorescence Parameters of the Dansyl Probe in Various Reference Solutions and in Reverse Micelles of L62 and L64 in *o*-Xylene as a Function of $W = [H_2O]/[EO]$; $\lambda_{ex} = 335$ nm[a]

system	*W*	λ_m, nm	λ_1, nm	λ_2, nm	I_1	τ_1, ns
TEG/H_2O	0	522.0	523.7			17.31
	0.5	526.7	524.4			15.64
	1.0	528.6	527.6			13.95
TGMME/H_2O	0	504.1	499.8	520.8		18.76
	2.0	529.0	527.9	519.1		13.33
TEGDME/H_2O	0	509.5	503.8	550.0		17.76
PPO	0	492.9	491.5	546.5		
o-xylene	0	489.5	490.3			
L62/*o*-xylene/H_2O	0	491.9	493.8	545.9	149.2	14.96
	0.1	493.5	495.9		145.8	14.41
	0.2	495.7	496.7	547.3	143.1	
	0.4	496.7	499.8	546.6	141.2	15.34
	0.5	496.9	499.1	546.1	139.7	15.29
	0.7	497.3	498.7	545.6	139.0	
	0.9	497.4	498.4	546.2	138.8	
	1.0	497.7	498.6	547.7	137.4	14.34
	1.5	496.6	498.4	548.0	135.6	
	2.0	496.3	497.9	545.9	134.6	13.55
	2.5	495.3	496.9	546.5	133.6	
	3.0	494.2	496.4	547.9	132.7	13.43
	3.9	493.9	495.9	545.8	131.6	
L64/*o*-xylene/H_2O	0.0	496.9	497.5	548.9	162.1	14.75
	0.1	497.6	498.3	546.6	163.8	13.92
	0.2	499.8	501.0	546.9	158.7	14.90
	0.5	501.0	501.4	549.2	151.1	13.72
	0.7	504.5	502.6	550.0	150.1	13.76
	1.0	502.3	501.3	547.0	149.5	13.79
	1.5	500.7	500.0	547.9	144.3	13.80
	2.0	499.2	499.1	543.8	140.6	13.75
L62/H_2O	1.0	510.9	510.6		780.3	
	2.0	512.5	511.7		393.2	
L64/H_2O	1.0	516.8	517.1		689.4	

[a] I_1 stands for the intensity of the first Gaussian band (with maximum at λ_1); τ was measured at $\lambda_{ex} = 295$ nm and $\lambda_{em} = 490$ nm.

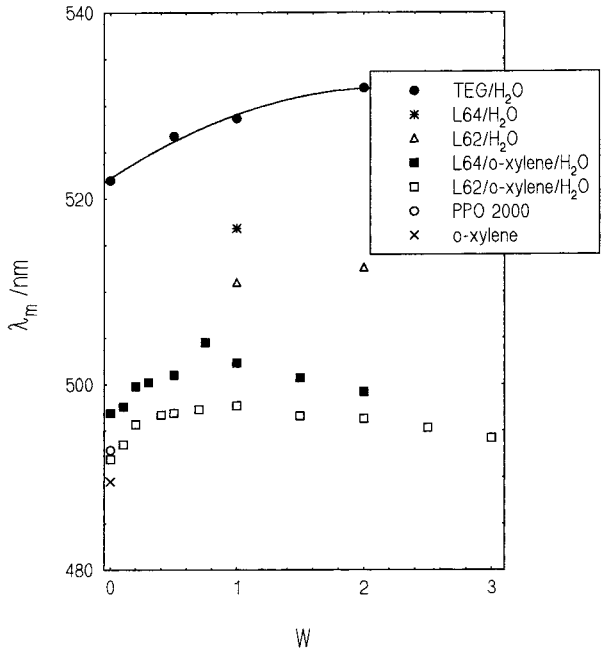

Figure 5. Plot of λ_m versus *W* for the Dansyl probe in various systems.

$= 0.1$) to 24.02 ($W = 0.4$). Regarding R_F, the differences noted in the two probes may be accounted for in terms of the intramolecular interactions of the substituents which are less important in Dansyl (1,5-substituted) than in ANS (*peri*-substituted). These interactions are hindered to a greater extent in the micellar aggregate, where the large Dansyl molecule is fixed. Thus, at least in the case of micellar solutions, one can consider that the fluorescence band is a single Gaussian; this is why R_F and I_2 are not listed in Table 2.

The fluorescence lifetime, τ, was measured at $\lambda_{em} = 490$ nm, and the experimental data were fitted with a sum of two exponentials, resulting in two lifetime values; the τ_2 values which are lying within the 1−2-ns range are not listed in Table 2. Regarding the variation of τ_1, it could be accounted for by resorting to the same reasoning as in the case of the λ shifts. At $W < 0.4$ for L62 and $W < 0.2$ for L64, the τ_1 values exceeded the values measured in *o*-xylene, indicating association of the probe with the polymers dissolved as unimers. It should be emphasized that τ_1 and, implicitly, the fluorescence intensity depend on polarity and viscosity; therefore, the value of τ_1 (as well as I_1) decreases when W increases; however, at $W = 0.4$ for L62 and 0.2 for L64, it takes a higher value, pointing to micellization. At $W > 0.7$, the decrease of τ_1 is very small. Comparison of the data presented in Tables 1 and 2 evidences a similar tendency; however, the decrease of fluorescence parameters with W is less important in the case of Dansyl probes, a behavior which is assigned to the different variations of the polarity at the location of these two probes.

Taking into account the variation of all Dansyl fluorescence parameters, one finds out the following for the ternary systems: (1) Micellization occurs at $W = 0.2$ for L64 and 0.4 for L62, the same values as those obtained with ANS. (2) The probe is located close to the PPO block, in a less polar region, as compared to ANS. (3) Due to the probe localization, the fluorescence parameters of Dansyl are less influenced by water addition as compared to ANS. (4) Starting at $W > 0.7$ for L64 and $W > 1.1$ for L62, a decrease of local polarity was observed, which was assigned to a better separation of the PPO−PEO blocks, when micellar organization progresses. (5) The polarity at the probe location is lower in L62 compared to L64 for the same W; a difference between L64 and L62 is not observed with ANS, in a more polar region.

For the binary L64/water and L62/water reverse micelles, the following information was obtained: (i) The polarity indicated by the probe is higher than in the ternary system with the same W. (ii) The polarity "sensed" by Dansyl increases with increasing water content (compare $W = 2$ with $W = 1$ in L62/water), indicating the presence of water at the probe location. In accord with this, the fluorescence intensity decreases considerably (Table 2), which pleads for the presence of water close to the probe and for the decreasing of the microviscosity. (iii) In L62/water, the probe reports a lower polarity compared to L64/water, as was also observed in the ternary systems.

PSA Probe. It is well-known that in the case of pyrene, frequently employed as a probe for direct micelles,[32−34] the fluorescence spectrum exhibits five vibrational bands. The first, located at 372.4 nm, is sensitive to polarity, its intensity increasing in polar solvents.[35] The third, located at 328.9 nm, does not practically vary with polarity, and therefore, the I_1/I_3 intensity ratio is considered to be a measure of the medium polarity. Pyrenesulfonic acid sodium salt, solubilized in the reverse micelles, exhibits a fluorescence spectrum having a vibronic structure similar to that of pyrene, the I_1/I_3 ratio also being dependent on the polarity of the microenvironment.[12,36] The first and the second bands overlap; thus, the fluorescence spectrum was fitted (over the 23 190−26 970-cm^{-1} range) with a sum of five Gaussian curves, using the Peakfit deconvolution program. After deconvolution of the spectrum, the five main bands, 376.8, 379.4, 387.2, 396.2, and 412.8 nm (Figure 6), were evidenced. Table 3 lists the values of the intensity ratios of various vibrational bands in the fluorescence spectrum of the probe in various media and the positions of the vibrational bands, λ_1 and λ_3. The variations with W of the three intensity ratios (Table 3) are similar: thus, for $W = 0.35-0.5$, a jump is recorded, the values almost reaching those of the TEG/water mixture. For $W > 0.5$, the ratios increase continuosly, yet to a lesser extent than in the calibration mixture. Regarding the positions of the vibrational bands, they are slightly shifted with W, as can be noted for λ_1 and λ_3 in Table 3. The intensity ratios in the TEG/water mixtures suggest that the PSA molecules are located in the poly(oxyethylene) region, in a more hydrophilic region as compared to Dansyl or ANS molecules. Accordingly, PSA also "senses" better the addition of water, by an almost continuous increase of the intensity ratios.

All these PSA fluorescence parameters confirm the role of water in the micellization process and show a variable increase of micropolarity with W at the location of the probe in the micelle, in the poly(oxyethylene) region.

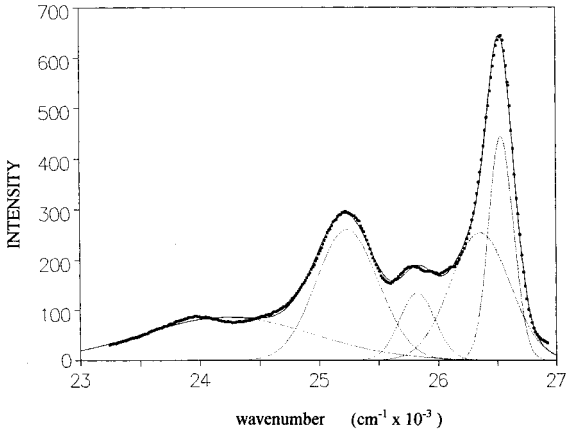

Figure 6. Deconvoluted fluorescence spectrum of PSA in the L62/*o*-xylene/water ($W = 0.5$) solution; $\lambda_{ex} = 329$ nm.

TABLE 3: Fluorescence Parameters of the PSA Probe in L62/*o*-xylene/H_2O, Compared to Those in the Reference TEG/H_2O Mixtures and Various Solvents; $\lambda_{ex} = 329$ nm

system	W	I_{377}/I_{388}	λ_1, nm	λ_3, nm	I_1/I_3	I_1/I_4	I_4
H_2O		4.25	376.1	386.1	3.386	1.915	
ethanol		3.47	375.8	386.3	3.340	1.696	
o-xylene		2.06	377.2	388.3	2.485	1.350	
TEG/H_2O	0	2.82	376.9	387.7	3.308	1.609	394.9
	0.25	3.04	376.8	387.3	3.326	1.645	470.8
	0.50	3.43	376.8	387.2	3.500	1.694	614.3
	1.0	3.74	376.7	387.1	3.610	1.739	673.1
	2.0	4.15	376.7	386.8	3.650	1.780	606.8
	3.0	4.22	376.7	386.7	3.855	1.787	600.4
L62/*o*-xylene/ H_2O	0	2.06	376.9	387.9	2.485	1.348	114.0
	0.1	2.08	376.9	387.9	2.733	1.389	128.5
	0.35	3.20	376.8	387.2	3.151	1.600	294.7
	0.50	3.39	376.8	387.2	3.351	1.682	313.8
	0.75	3.50	376.8	387.2	3.360	1.710	314.0
	1.0	3.52	376.8	387.2	3.366	1.715	314.3
	2.0	3.56	376.7	387.1	3.380	1.719	314.6
	3.0	3.68	376.7	387.1	3.389	1.722	315.2
L62/H_2O	1.0	2.91	376.7	386.7	3.05	1.55	
	2.0	3.29	376.6	386.6	3.27	1.67	

TABLE 4: Dependence of λ_{max} of the NP Probe on Water Content, *W*, in Reverse Micellar Solutions of L62 and L64 and in Reference Systems

L62/*o*-Xylene/H_2O													
W	0.01	0.30	0.50	1.00	1.30	1.50	2.00	2.50	3.00	3.50	3.70	3.80	3.90
λ_{max}	352.0	351.7	351.5	351.0	350.4	349.5	347.8	345.5	344.2	343.0	342.5	342.0	341.6
L62/H_2O													
W	0.01	0.50	1.00	1.50	2.00								
λ_{max}	352.0	348.3	345.5	342.0	338.0								
L64/*o*-Xylene/H_2O													
W	0.03	0.30	0.50	0.60	1.00	1.20	1.50	1.75	1.90	2.00	2.30		
λ_{max}	352.0	350.6	349.7	349.2	347.5	346.5	345.0	344.0	343.0	342.5	341.0		
L64/H_2O													
W	0.01	0.20	0.50	1.00									
λ_{max}	352.0	349.0	346.0	341.6									
TEG/H_2O													
W	0.03	0.25	0.50	0.75	1.00	1.25	1.50	1.75	2.00	3.00	4.00		
λ_{max}	344.0	341.0	337.4	335.0	333.2	331.4	329.0	327.2	325.8	322.3	320.4		
TGMME/H_2O													
W	0	0.20	0.50	0.75	1.00	1.50	2.00						
λ_{max}	350.0	347.4	343.7	341.2	339.0	335.7	333.1						
TEGDME/H_2O													
W	0	0.20	0.50	1.00	1.50	2.00							
λ_{max}	354.0	351.1	347.6	342.9	339.9	337.0							

The variation of the fluorescence intensity at 396 nm (I_4 in the PSA fluorescence spectrum) with *W* (Table 3) evidences the micellization at $W = 0.35-0.4$, in the case of the L62/*o*-xylene system, by a strong increase of the fluorescence intensity, probably owing to better shielding of the probe in organized aggregates.

For the binary L62/water reverse micelles, the polarity indicated by PSA is lower than in the ternary systems with the same *W* (Table 3). The effect sensed by this polar probe is opposite to those recorded by the more hydrophobic probes, ANS and Dansyl. Thus, in binary systems, the water seems to be more uniformly distributed as compared to the corresponding ternary systems.

UV−Vis. *NP Probe.* The 4-nitropyridine *N*-oxide (NP) molecular probe is water-soluble and only slightly soluble in nonpolar solvents, its partition coefficients for water/*o*-xylene and water/cyclohexane being higher than 1500. The spectrophotometric properties of the NP probe in the UV−vis region and its negative solvatochromie are known.[37] Upon solvent polarity increase, the $\pi \rightarrow \pi^*$ absorption band shifts hipsochromically (e.g., λ_{max} is at 350 nm in acetone, 333 nm in methanol, and 314 nm in water). In polar solvents, the ground state of the NP molecule is stabilized and the transition energy increases, which brings about the blue shift of the absorption maximum. In protic solvents, the hydrogen bonds which imply the N−O group play an important role in NP solvatochromism. In the solvents that do not form hydrogen bonds, the small hypsochromic shifts of the absorption maximum are determined by dipole−dipole interactions.[37]

Spectral absorption measurements of NP in various solvents have shown that its transition energies, E_{NP}, can be utilized as a polarity parameter similar to Kosower's *Z* values[38] (transition energies corresponding to the charge-transfer bands of 1-ethyl-4-carbomethoxypyridine iodide). Thus, a good linear relationship between E_{NP} and *Z* has been observed for NP,[14] as described by the equation $Z = 3.008E_{NP} - 178.4$, where E_{NP} and *Z* are expressed in kilocalories/mole. We have successfully used this relationship for measuring the micropolarity in Triton X-100 reverse micelles.[14]

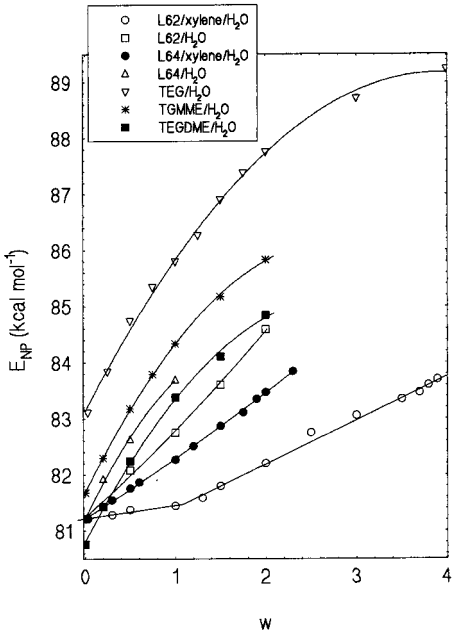

Figure 7. E_{NP} dependence on *W* in the L62/*o*-xylene/water, L62/water, L64/*o*-xylene/water, L64/water, and reference systems.

In L62 and L64 micellar systems, the absorption spectra of NP show a hipsochromic shift with increasing amount of water, pointing to an increase of the micropolarity in the NP location zone.

To interpret the E_{NP} values in terms of water distribution inside the polar core of the L62 and L64 micelles, calibration measurements on a series of TEG/water, TGMME/water, and TEGDME/water homogeneous mixtures were used.

Data in Table 4 and Figure 7 show that in "dry" solutions of L62/*o*-xylene and L64/*o*-xylene or in pure L62 and L64 surfactants, the probe showed identical polarities, smaller than those of TEG and TGMME and equivalent to those of the TEGDME/water mixture with $W = 0.15$. On addition of water in the surfactant/*o*-xylene solutions, the polarity at the NP location increases slightly in both surfactant systems, remaining lower than that of the TEG/water and TGMME/water reference systems, with the same *W*, and comparable to that of the

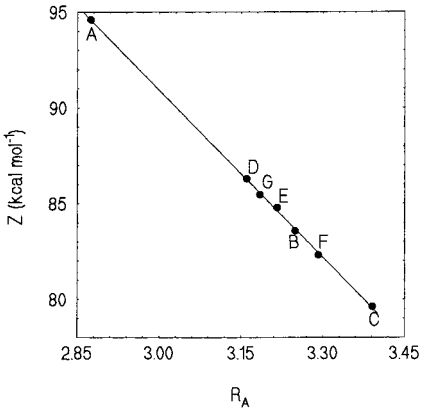

Figure 8. Correlation between the values of Kosower's Z and R_A of the PSA probe: water (A), methanol (B), ethanol (C), 70% v/v aqueous ethanol (D), 80% v/v aqueous ethanol (E), 90% v/v aqueous ethanol (F).

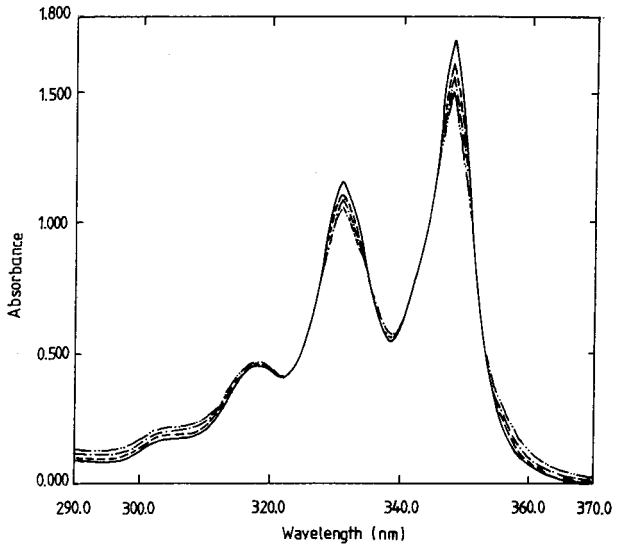

Figure 9. UV−vis absorption spectra of the PSA probe in L62/*o*-xylene/water with various concentrations: $W = 0$ (—), 0.5 (− −), 1.5 (−·−), and 3.5 (−··−).

TEGDME/water mixtures. This places NP at the periphery of the polar core. At the same amount of water, W, in the system, the micropolarity measured by NP is higher in the L64 reverse micelles than in the L62 ones. The polarity increases in both systems, and finally, at $W = 2.3$ for L64/*o*-xylene and at $W = 3.9$ for L62/*o*-xylene, the E_{NP} values are almost identical and correspond to the value found for the TEG/water mixture with $W = 0.25$. One can conclude that the higher the EO/surfactant ratio, the higher the local micropolarity at the same water content; e.g., at $W = 2.0$ for L64/*o*-xylene (with 37.65% g/g EO/surfactant), $E_{NP} = 83.47$ kcal mol^{-1}, against L62/*o*-xylene (with 19.4% g/g EO/surfactant) whose E_{NP} is 82.2 kcal mol^{-1}.

In the binary L64/water and L62/water systems, NP senses higher polarities than those of the ternary systems with the same W values (Table 4, Figure 7), as was observed with Dansyl and ANS.

PSA Probe. The absorption spectrum of this probe has a resolved vibrational structure, the ratios of the absorbances changing when the polarity of the medium varies. The ratio of absorbances at 348 and 317 nm (denoted by R_A) was selected as a measure of the polarity; it increases with a decrease of the solvent polarity. Thus, $R_A = 2.874$ in water, 3.391 in ethanol, and 3.663 in TEG. Figure 8 shows the linear dependence of Z on R_A for water, ethanol, and ethanol/water mixtures. The linear correlation obtaining $Z = -29.0R_A + 177.83$ allows the use of this ratio as a polarity parameter. For the TEG/water calibration mixtures, the same Z versus W curve is obtained as with NP (see Figure 14), which represents an important internal check of the methodology. The absorption spectra of the PSA probe in the reverse micellar systems of L62/*o*-xylene with various W are presented in Figure 9. Table 5 shows the dependence of R_A on W for the ternary L62 system and for the TEG/water mixtures. The hydration values at the location of PSA are within the range of TEG/water reference values. The data in Tables 4 and 5 clearly indicate that the PSA probe is located in a more hydrated region of the L62 reverse micelle than is the NP probe.

ESR. *Cationic Spin Probes, CAT n.* In the homologous series of cationic probes, the identical nitroxide moiety ensures that a_N values vary only as a result of different surroundings. The probes positioning is a result of the fine balance of the interactions of the cationic head and of the hydrocarbon chain "tail". Since the head is always the same and the tail increases in a regular fashion with n, the relative positioning of the probes is defined in a straightforward way: CAT 1 will be solubilized in the most polar part, and as the hydrocarbon chain increases, the average position of the probes will shift further and further toward the hydrophobic region.

Polarity Profile. The ESR spectra of the homologous CAT n series ($n = 1$, 4, 8, 11, and 16) were measured, and a_N, the polarity-sensitive parameter, was determined. A calibration of a_N values as a function of the water content in PEO was accomplished by using the previously measured calibration curve of CAT 4 in TEG/water mixtures with different W values.[12,16]

Parts a and b of Figure 10 show the ESR spectra of CAT n in the L62/*o*-xylene/water systems with $W = 0.4$ and $W = 2$, respectively. The polarity changes with W for L62 micellar solutions, as can be seen in Table 6. As in the case of L64/*o*-xylene/water,[16] in the range of water concentrations studied, the system exhibits a complete polarity profile, the a_N values differing from one probe to the other: e.g., it ranges from 16.25 G (CAT 1) to 15.55 G (CAT 16) in the case of L62/*o*-xylene/water with $W = 0.4$. Comparison of L62 and L64 ternary systems evidences some differences in the a_N values, although they generally have similar behavior.

A comparison of the ternary and binary systems with the same surfactant shows that CAT 1, CAT 4, and CAT 8 probes "sense" a higher local polarity in the ternary systems, indicating a more advanced segregation of water in the ternary systems.

Taking a_N as an index of hydration, the effective degree of hydration, W_{eff}, at the probe site[14,16] was deduced from a calibration curve of a_N versus W in the reference (TEG/water) mixtures. The W_{eff} versus W graphs for the two L62 systems

TABLE 5: R_A Ratios of the PSA Probe versus the Water Content, W, in L62/*o*-xylene/H_2O and in TEG/H_2O

						L62/*o*-Xylene/H_2O							
W	0	0.1	0.2	0.5	0.75	1.0	1.5	2.0	2.5	3.0	3.5	3.7	3.8
R_A	3.613	3.591	3.577	3.539	3.511	3.480	3.411	3.339	3.266	3.187	3.091	3.051	3.028
						TEG/H_2O							
W	0	0.75	1.5	2.5									
R_A	3.663	3.460	3.287	3.132									

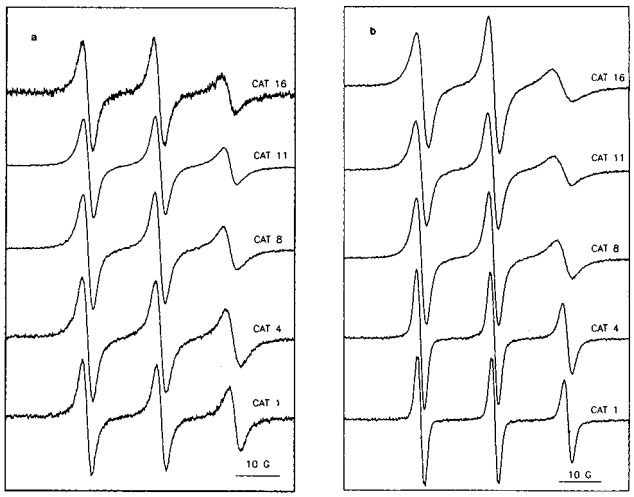

Figure 10. ESR spectra of CAT *n* spin probes in L62/*o*-xylene/water with (a) $W = 0.4$. and (b) 2.

TABLE 6: Isotropic ^{14}N Hyperfine Splittings, a_N (G), of CAT *n* Spectra in Reverse Micelles of L62/*o*-xylene/Water and L62/ Water, as a Function of Water Content, *W*, at 295 K

W	CAT 1	CAT 4	CAT 8	CAT 11	CAT 16
		L62/*o*-Xylene/Water, 295 K			
0.40	16.25	16.00	15.63	15.54	15.55
1.00	16.33	16.25	15.90	15.68	15.65
2.00	16.48	16.37	16.04	15.90	15.60
		L62/Water, 295 K			
1.00	16.05	16.00	15.75	*a*	*a*
2.00	16.25	16.10	16.05	*a*	*a*

[a] Not determined; a_N values for CAT 4 (at 320 K) are 16.75 G in water, 15.65 G in Carbowax 300, 15.34 G in PPO, 15.33 G in TEGDME, and (at 300 K) 15.30 G in *o*-xylene.[25]

(Figure 11) emphasize the differences in local hydration values reported by the five CAT *n* probes: (i) in the ternary system, CAT 1 and CAT 4 sense a local hydration higher than in the reference system with the same *W*, while probes CAT 8, CAT 11, and CAT 16 indicate lower hydration, and (ii) in the binary systems, the local hydration values found by all CAT *n* probes are smaller than those in the reference system with the same *W*. For a more complete description of the hydration profile, W_{eff} data for other probes were represented on the same figure.

Rotational Correlation Times, τ_c. The τ_c dependence on *W* reflects the microviscosity modifications (Figure 12), which are thought to result from the water distribution. One can distinguish two regions in both ternary systems studied: one toward the center of the polar core, where the viscosity decreases (τ_c for CAT 1 and CAT 4 decreases after the initial increase of τ_c at $W = 0.25$, when the micelles are formed[16]) with increasing water content, and a second, peripheral region of the polar core, where τ_c (and the microviscosity) increases with *W*, more effectively in the case of L62.

The τ_c values are larger in the binary mixtures than in the ternary systems at the same *W*. CAT 1, CAT 4, and CAT 8 sense microviscosities in the hydrophilic zone, larger in L62/water than in L64/water. These results agree with the lower hydration degrees in L62/water, as supplied by the variation of the a_N values. Much larger τ_c values for the binary as compared to ternary systems, at the same *W*, were also found with the 16-doxyl spin probe (Table 7 and Table 8), the monitoring group being in this case shifted farther toward the hydrophobic region of the micelle in comparison to the above CAT *n* spin probes. This result gives more consistency to the microviscosity differences between binary and ternary systems at the same *W*.

Doxylstearic Acid Spin Probes. Order Degree and Profile. The *x*-doxylstearic acid probes ($x = 5$, 7, 10, and 16) were used to measure the order degree of the surfactant chains as well as the solvent penetration into the micellar shell.[12,14,16,25] The experimental parameters followed were a_N and τ_c for the isotropic spectra and $A_{||}$ and $A_{\perp}$ for the anisotropic spectra, from which the order parameter, *S*, can be calculated. Figure 13 shows typical *x*-doxyl spectra in the reverse micelles of the ternary and binary L62 systems with $W = 2$.

The parameters of the anisotropic spectra in the ternary L62 system (Table 7) show that the motion becomes less restrained as the doxyl group is further from the COO^- group. For 16-doxyl, the motion is completely isotropic. The a_N value for this probe is equal to either the value found in PPO and the value found in the solvent (*o*-xylene). Unfortunately, this coincidence does not allow us to evaluate the solvation at the probe location, which is not at the limits of the corona. However, at a lower *W* value ($W = 1$), the spectrum is broadened by CuX_2, while at a higher *W* value ($W = 2$) the spectrum is not affected. This is an indication that at higher water content, the corona of the micelle is more compact and cannot be penetrated by the broadening reagent. This result is also strengthened (i) by the trend of the order parameter values to increase with increasing water content (Table 7) and (ii) by the similar dependence on the water content of the microvis-

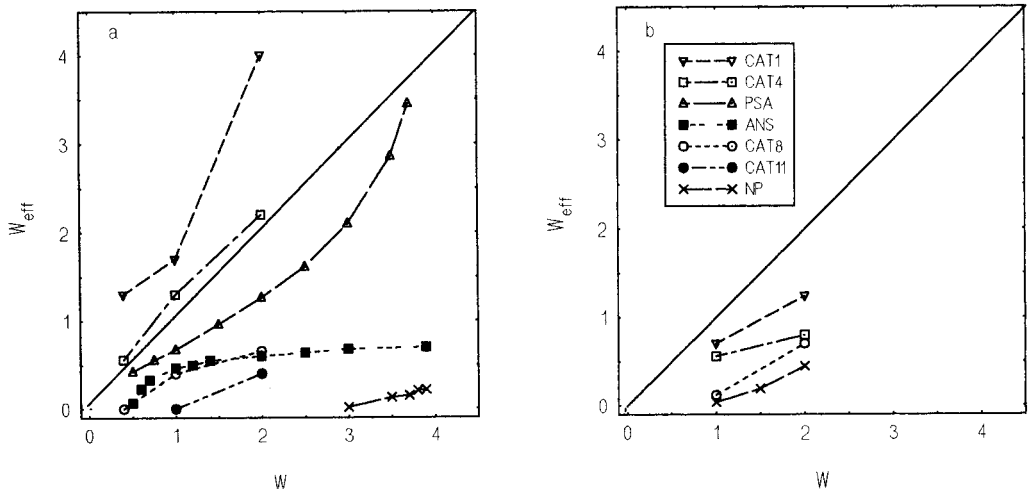

Figure 11. Plot of the effective degree of hydration W_{eff} versus *W* in (a) L62/*o*-xylene/water and (b) L62/water.

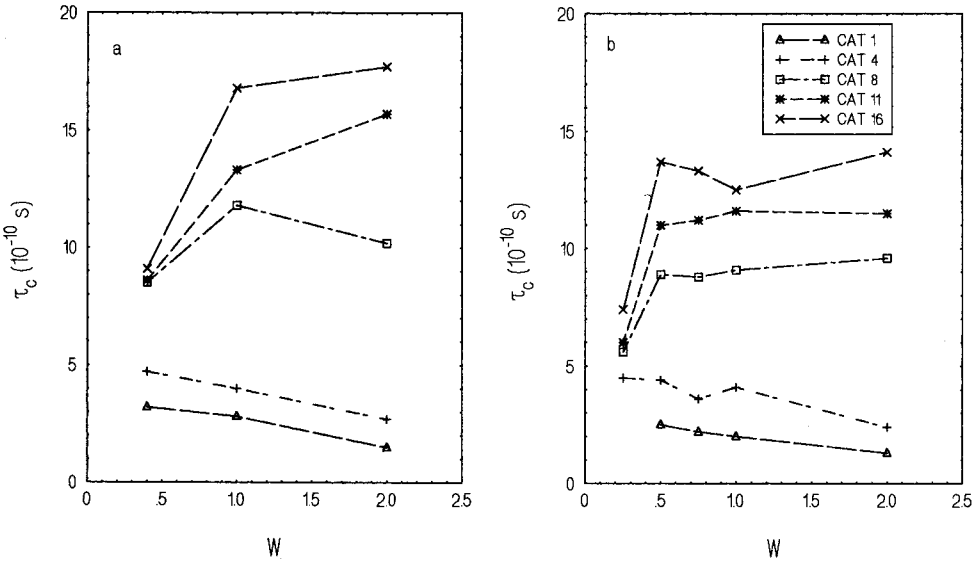

Figure 12. Plot of τ_c versus W for the CAT n spin probes in (a) L62/*o*-xylene/water and (b) L64/xylene/water.

TABLE 7: ESR Parameters of *x*-Doxylstearic Acid Spin Probes in Reverse Micelles of L62/*o*-Xylene/Water as a Function of *W*, at 295 K

W	probe	$A_{\|\|}$, G	$A_\perp$, G	a_N, G	τ_c, 10^{-10} s	S
0.5	5-doxyl			14.3[a]	7.0	
1.0	5-doxyl	22.0	10.8	14.5[b]		0.43
	7-doxyl	20.6	11.2	14.3[b]		0.36
	16-doxyl			14.3[a,c]	1.8	
2.0	5-doxyl	22.4	10.9	14.7[b]		0.43
	7-doxyl	20.8	11.3	14.5[b]		0.36
	10-doxyl	17.7	12.1	14.0[b]		0.22
	16-doxyl			14.3[a]	2.7	
PPO	16-doxyl			14.3[d,e]	~14.5[d]	
o-xylene	16-doxyl			14.3[a]	1.1	

[a] Measured directly. [b] Calculated as $1/3(A_{||} + 2A_\perp)$. [c] Broadened by CuX_2. [d] At 295 K, slightly anisotropic spectrum. [e] Measured at 340 K.

cosity (τ_c values) monitored around 16-doxyl. Thus, the micelles appear to be better organized at higher amounts of solubilized water, with order extending further and with the corona becoming less penetrable. At the same W, a decrease of order from the polar core toward the corona is found.

Regarding the ordering (S), microviscosity (τ_c), and penetrability in the L62 ternary system, these structural parameters seem to be almost identical to those of the L64 system,[16] a slight increase in ordering being observed for the L62 system, which might be correlated with a longer PPO chain in this copolymer in comparison with its size in L64.

For the binary systems, at 295 K, the shape of the spectra (Figure 13b) corresponds to a slowing down of the rotation around the long molecular axis of the probe,[40,41] irrespective of the doxyl group position. The $A_{||}$ values (Table 8) do not follow the decreasing order 5-doxyl > 7-doxyl > 10-doxyl > 16-doxyl measured for the ternary systems, which is indicative for an order profile. It has been shown[40,41] that when the rate of the spin probe rotational diffusion decreases under a certain limit, the order parameter formalism can no longer be used. Therefore, in this case, values for S and a_N have not been calculated. The "freezing" of the polymer chains mobility at a rather high temperature (295 K) has been observed also in the case of the direct micelles of Pluronic P85[39] and of a "conventional" surfactant with long PEO chains (Triton X-100).[42] Unlike the latter systems, in the reversed binary systems studied here, containing a very low amount of water, the temperature increase to 320 K does not lead to sufficient chain mobility for an order parameter to be determined (see the $A_{||}$ values for the *x*-doxyl series in Table 8). The observation that, in the ternary systems, both the order parameter and the order profile can be measured clearly points to the role of the solvent (*o*-xylene) in determining a loose packing of the PPO chains in the corona, this effect being also felt in the PEO polar core.

TABLE 8: ESR Parameters of the Anisotropic Spectra of *x*-Doxylstearic Acid Probes in Binary L62/Water and L64/Water Systems

probe	$A_{\|\|}$, G	$A_\perp$, G	a_N, G	τ_c (10^{-10} s)
		295 K		
		L62, $W = 1$		
5-doxyl	24.7	9.3	*a*	
7-doxyl	28.4	9.1	*a*	
10-doxyl	27.5	9.1	*a*	
16-doxyl	*b*	*b*	*b*	~17.5[b]
		L62, $W = 2$		
5-doxyl	25.1	9.4	*a*	
7-doxyl	28.6	9.0	*a*	
10-doxyl	27.7	9.3	*a*	
16-doxyl	*b*	*b*	*b*	~17.5
		L64, $W = 1$		
5-doxyl	25.1	9.4	*a*	
7-doxyl	28.5	8.9	*a*	
10-doxyl	27.3	9.2	*a*	
16-doxyl	*b*	*b*	*b*	~17.2
		310 K		
		L62, $W = 1$		
5-doxyl	~20.1	11.0	*a*	
7-doxyl	26.4	10.3	*a*	
10-doxyl	~26.2	10.6	*a*	
16-doxyl			14.4[c,d]	8.4
		L64, $W = 1$		
5-doxyl	23.0	10.4	*a*	
7-doxyl	25.9	10.0	*a*	
10-doxyl	~25.1	10.4	*a*	
16-doxyl			14.4[c,d]	9.4
		320 K		
		L64, $W = 1$		
5-doxyl	21.5	11.1	*a*	
7-doxyl	~22.8	10.7	*a*	
10-doxyl	*e*	*e*	*a*	
16-doxyl			14.4[c,d]	5.3

[a] Not calculated (see text). [b] Slightly anisotropic spectra. [c] Isotropic spectra. [d] Measured directly. [e] Anisotropic spectrum without $A_{||}$ features.

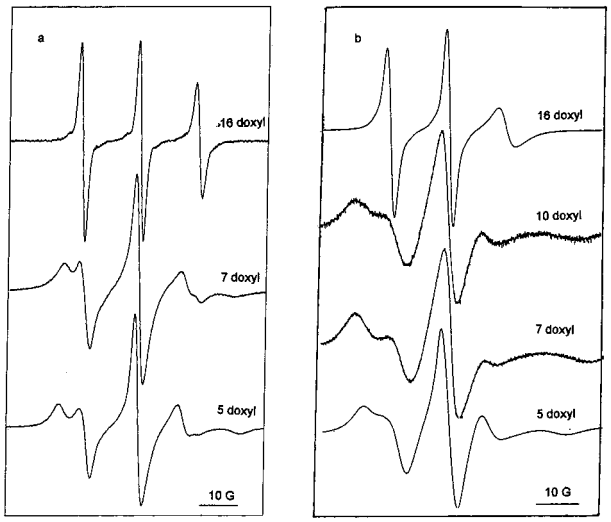

Figure 13. ESR spectra of *x*-doxylstearic acid probes in (a) L62/*o*-xylene/water ($W = 2$) and (b) L62/water ($W = 2$).

Results Relating to Kosower's *Z* Polarity Scale. To achieve the relative location of the probes and to refer all results to a common, more general scale of polarities, the specific parameters of the three spectral methods used were "converted" into values of Kosower's polarity factors, *Z*, for the L62 systems (Figure 14). Use has been made of the *Z* versus *W* calibration curve obtained for TEG/water mixture with NP probe[14] and with PSA, as well as of the calibration curves describing the dependence of the specific parameters (values listed in the tables) on *W*, to obtain the *Z* versus *W* values for the probes in the micellar solutions. It is worth mentioning that for Dansyl, lying in a zone of high hydrophobicity, the conversion into *Z* values was not possible. The probes CAT 1 and CAT 4 experience a higher polarity than that of the TEG/water mixture, at the same *W*, similar to those in the ethanol/water mixture ($Z_{ethanol} = 79.6$ kcal mol^{-1}, $Z_{water} = 94.6$ kcal mol^{-1}). The other probes indicate lower polarities than the TEG/water mixture, while CAT 16 and the NP probes sense even lower polarities than TEG. The span of *Z* values ranges from 66.7 (NP) to 84.2 kcal mol^{-1}(CAT 1). In the binary systems, hydration is more uniform, the hydrophilic probes show lower polarities, and the hydrophobic ones show higher polarities, while CAT 8 yields almost the same results as in the ternary system. In this case, the range of *Z* values is reduced to above half of the above one, i.e., from 70.3 (NP) to 77.8 kcal mol^{-1} (CAT 1). Regarding the similar systems of L64 (converting local hydration values[16] into *Z*), the range of *Z* values appears shifted toward higher polarities: in the ternary system with $W = 1$, $Z = 69.2$ (NP) and 87.4 kcal mol^{-1} (CAT 1), while in the binary system $Z = 73.1$ (NP) and 80.4 kcal mol^{-1} (CAT 1).

Conclusions

The spectral measurements carried out on a wide range of molecular probes with various locations resulted in complementary and concordant conclusions regarding micellization, hydration (polarity), and microviscosity in various micellar zones at water addition, as follows:

1. Water is a prerequisite for micellization, the fluorescent probes yielding the same minimal water quantity required for micellization: $W = 0.4$ for L62/*o*-xylene and $W = 0.2$ for L64/*o*-xylene, in agreement with the spin probe results for L64.[16] These two *W* values represent the same weight percent concentration, *i.e.*, 1.1% of water. A number of different experimental data[43] also show that the L62 and L64 solutions present a very close resemblance when compared at the same w/w % concentration. A possible explanation should consider the lengths of the hydrated parts of the two copolymers much closer than suggested by their formulas.

2. In the binary L62/water systems in the L_2 phase, similarly with L64,[16] the probes have evidenced a polarity gradient (Figure 14b), indicating the segregation of the polar parts of the amphiphilic block-copolymers in the presence of water. By extension, these structures can be assimilated with reverse micelles.

3. It was found that the R_A parameter of PSA (in the absorption spectra) has a linear correlation with Kosower's *Z*

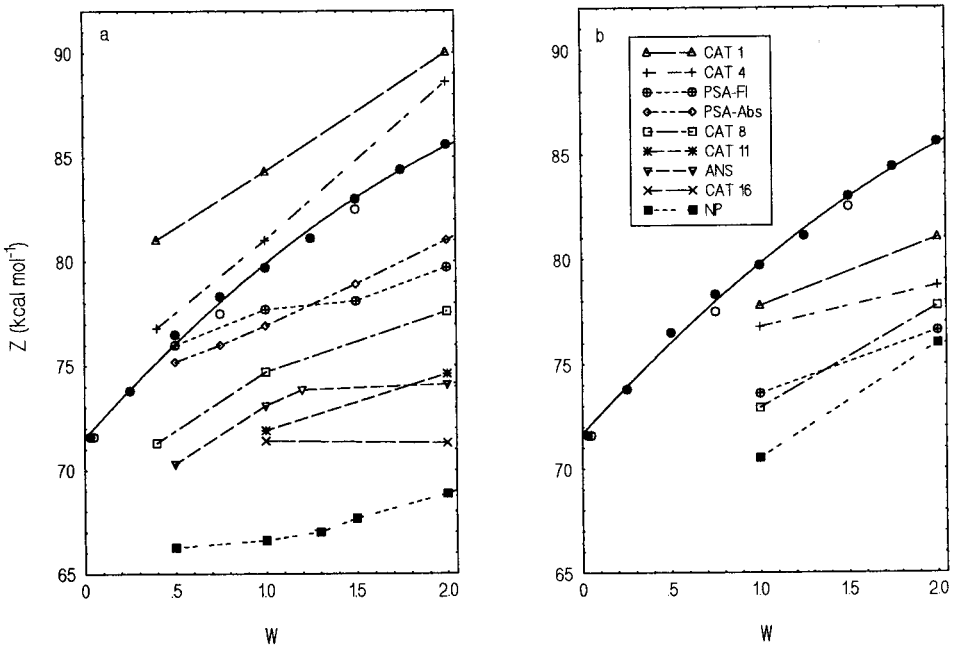

Figure 14. Kosower's *Z* values in reverse micelles of (a) L62/*o*-xylene/water and (b) L62/water as a function of *W*, at the location of the different spin, fluorescence, and UV−vis probes; the continuous line represents the calibration curve, obtained with the NP (●) and PSA probes (○) by UV−vis determinations in the TEG/water mixtures.

in ethanol/water mixtures ($Z = -29.0R_A + 177.83$). Using this equation, Z values were assigned to the TEG/water mixtures, which agreed perfectly with earlier determinations, when the NP probe transition energy was employed for callibration.[14]

4. The hydration gradient in the core was determined for the L62 reverse micelles, the range of W_{eff} values being much larger in the presence of the nonpolar solvent.

5. The values of the polarity-sensitive parameters of most probes in the reverse micelles have also been "translated" into values of Kosower`s Z polarity factor. In this way, an ordering of all probes used was achieved, according to their hydrophobe character: Dansyl > NP > CAT 16 > CAT 11 ~ ANS > CAT 8 > PSA > CAT 4 > CAT 1.

6. Segregation of water is more advanced in the ternary systems than in the corresponding binary ones, the range of Z values being double in the first case as compared to the second one, which points to the influence of the nonpolar solvent on water distribution.

7. Microviscosity data confirm the hydration profile, since an increase of the water content brings about a decrease of the microviscosity in the middle of the core and an increase at the polar/nonpolar interface.

8. The microviscosity is much lower in the ternary than in the binary systems at the same water content, owing to the considerable solvation of the PPO region, which determines a looser packing of surfactant chains, even in the PEO core.

9. Water contributes to the micellar ordering. For $W \geq 1$, a considerable order at the polar/apolar interface and a tighter packing in the corona were noted in both L62 and L64 ternary systems.

10. The structural characteristics of the L62 and L64 ternary systems are rather similar, a conclusion suggested especially by the information polar probes supplied. There are differences in the microenvironment of more hydrophobic probes, e.g., Dansyl and CAT 16 which sense higher hydrophobicities in case of L62. The increase of microviscosity is also more marked in L62.

Acknowledgment. This contribution is a result of a cooperation program between the Romanian Academy and the Academy of Finland. Financial support from the Romanian Academy (Grants 110/1996 and 287/1997) is gratefully acknowledged

References and Notes

(1) Almgren, M.; Brown, W.; Hvidt, S. *Colloid Polymer Sci*. **1995**, *273*, 2.
(2) Alexandridis, P. *Curr. Opinion Colloid Interface Sci.* **1996**, *1*, 490.
(3) Chu, B.; Zhou, Z. *Surfactant Sci. Ser*. **1996**, *60*, 67.
(4) Alexandridis, P.; Hatton, T. A. *Colloid Surf. A* **1995**, *96*, 1.
(5) Wu, G.; Chu, B. *Macromolecules* **1994**, *27*, 1766.
(6) Wu, G.; Zhou, Z.; Chu, B. *Macromolecules* **1993**, *26*, 2117.
(7) Alexandridis, P.; Olsson, U.; Lindman, B. *Macromolecules* **1995**, *28*, 7700.
(8) Alexandridis, P.; Olsson, U.; Lindman, B. *Langmuir* **1996**, *12*, 1419.
(9) Wu, G.; Zhou, Z.; Chu, B. *J. Polym. Sci. Polym. Phys. Ed.* **1993**, *31*, 2035.
(10) Ravey, J. C.; Buzier, M.; Picot, C. *J. Colloid Interface Sci.* **1984**, *97*, 9.
(11) Christenson, H.; Friberg, S. E.; Larsen D. *J. Phys. Chem.* **1980**, *84*, 3633.
(12) Caldararu, H.; Caragheorgheopol, A.; Vasilescu, M.; Dragutan, I.; Lemmetyinen, H. *J. Phys. Chem.* **1994**, *98*, 5320.
(13) Vasilescu, M.; Caragheorgheopol, A.; Almgren, M.; Brown, W.; Alsins, J.; Johannsson, R. *Langmuir* **1995**, *11*, 2893.
(14) Caragheorgheopol, A.; Bandula, R.; Caldararu, H.; Joela, H. *J. Mol. Liq.* **1997**, *72*, 105.
(15) Wu, G.; Chu, B.; Schneider, K. D. *J. Phys. Chem.* **1994**, *98*, 12018.
(16) Caragheorgheopol, A.; Pilar, J.; Schlick, S. *Macromolecules* **1997**, *10*, 2923.
(17) Wanka, G.; Hoffmann, H.; Ulbricht, W. *Macromolecules* **1994**, *27*, 4245.
(18) Hecht, E.; Mortensen, K.; Hoffmann, H. *Macromolecules* **1995**, *28*, 5465.
(19) Schmolka, R. In *Nonionic Surfactants*; Schick, M. J., Ed.; Marcel Dekker: New York, 1967; Chapter 10.
(20) Alexandridis, P.; Andersson, K. *J. Phys. Chem.* **1997**, *101*, 8103.
(21) Knauer, B. R.; Naples, J. J. *J. Am.Chem. Soc*. **1976**, *98*, 4395.
(22) Stone, T. J.; Buckman, T.; Nordio, P. L.; McConnell, H. M. *Proc. Natl. Acad. Sci. U.S.A.* **1965**, *54*, 1010.
(23) Seelig, J. In *Spin Labeling I*; Berliner, L. J., Ed.; Academic: New York, San Francisco, London, 1976; p 373.
(24) Gafney, B. J. In *Spin Labeling I*; Berliner L. J., Ed.; Academic: New York, San Francisco, London, 1976; p 567.
(25) Caldararu, H.; Caragheorgheopol, A.; Dimonie, M.; Donescu, D.; Marinescu, M. *J. Phys. Chem.* **1992**, *96*, 7109.
(26) Slavik, J. *Biochim. Biophys. Acta* **1982**, *1*, 694.
(27) Kosower, E. M.; Tanizawa, K. *Chem. Phys. Lett.* **1972**, *16*, 419.
(28) Penzer, G. R. *Eur. J. Biochem.* **1972**, *25*, 218.
(29) Balasubramaniayan, V. *Chem. Rev.* **1966**, *66*, 567.
(30) Turner, D. C.; Brand, L. *Biochemistry* **1968**, *7*, 3381.
(31) Li, Y. H.; Chan, L. M.; Tyer, L.; Moody, R.; Himel, C. M.; Hercules, D. M. *J. Am.Chem. Soc*. **1973**, *97*, 3118.
(32) Almgren, M. In *Kinetics and Catalysis in Microheterogeneous Systems*; Gratzel, M., Kalyanasundaram, K., Eds.; Marcel Dekker: New York, 1991; p 63.
(33) Vasilescu, M.; Anghel, F. D.; Almgren, M.; Hansson, P.; Saito, S. *Langmuir* **1997**, *13*, 6951.
(34) Feitosa, E.; Brown, W.; Vasilescu, M.; Swanson-Vethamuthu, M. *Macromolecules* **1996,** *29*, 6837.
(35) Kalyanasundaram, K.; Thomas, J. K. *J. Am.Chem. Soc*. **1977**, *99*, 2039.
(36) Verbeeck, A.; Gelade, E.; De Schryver, F. C. *Langmuir* **1986**, *2*, 448.
(37) Kubota, T.; Yamakowa, M. *Bull. Chem. Soc. Jpn*. **1962**, *35*, 555.
(38) Kosower, E. M. *J. Am.Chem. Soc.* **1958**, *80*, 3253.
(39) Caragheorgheopol, A.; Caldararu, H.; Dragutan, I.; Joela, H.; Brown, W. *Langmuir* **1997**, *13*, 6912.
(40) Mason, R. P.; Polnaszek, C. F.; Freed, J. H. *J. Phys. Chem.* **1974**, *78*, 1324.
(41) Cannon, B.; Polnaszek, C. F.; Butler, K. W.; Eriksson L. E. G.; Smith, I. C. P. *Arch. Biochem. Biophys.* **1975**, *167*, 505.
(42) Caldararu, H.; Caragheorgheopol, A. To be published.
(43) Caragheorgheopol, A.; Schlick, S. *Macromolecules*, submitted for publication.